DRY SPOT RADIUS AND MICROFILM THICKNESS BENEATH A VAPOR BUBBLE

M. G. Verdiev and S. A. Ninalalov

UDC 621.1.013

A simplified mechanism of energy supply to a bubble growing in a heterogeneous system is considered. The model described is based on approximate mass and energy balance equations for the evaporating portion of the microfilm and the vapor in the bubble. It will be assumed that the energy demand through the interphase boundary of the bubble cupola and the remaining portion of the microfilm can be neglected. Solutions of the equations presented satisfactorily describe available experimental data on microfilm thickness and dry spot radius.

Despite numerous studies of the growth of a vapor bubble in liquid boiling in a heterogeneous system, at present there is still no unified approach to the energy supply mechanism. Some investigators have commenced from the position that energy supply into a bubble growing on the heat liberation surface is accomplished conductively through the cupola [1, 2], while others have proposed that heat is supplied primarily through the interphase boundary at the periphery of the bubble's base [3], and a third group considers both mechanisms [4, 5], while the equations of bubble growth contain undefined constants, the values of which must be refined empirically.

The models described in [1, 2], obtained from consideration of bubble growth in a homogeneous system, together with attempts of some researchers to apply them to description of the bubble growth process on the heat liberation surface have not produced reliable results and lead to distortions of the kinetics of the phenomenon.

The voluminous data presented in [1-13] indicate that during bubble growth on a heat liberation surface a liquid microfilm and dry spot are formed beneath the bubble. In connection with this, the bubble energy supply mechanism described in [3] should be considered closest to the real pattern of the phenomenon. However, in this model it is assumed that the film through which energy supply occurs is formed only at the periphery of the bubble base, with its mean thickness ($\sim 20^{-4}$ m) being much greater than the thickness of a real microfilm. The inner radius of the microlayer in [3] corresponds to the outer radius of the microfilm.

Moreover, the majority of bubble growth equations have been obtained by consideration of only mechanical forces, or thermal processes alone, or else are based on hypothetical heat liberation mechanisms without any corresponding justification. As a result, the equations now available describe bubble behavior only over limited intervals of change of the system thermodynamic parameters.

The present study will consider a mechanism of energy supply to a bubble growing on a heat liberation surface which most adequately corresponds to the actual phenomenon.

Heat-mass exchange in liquid boiling on a heating surface is defined by the mechanisms of heat liberation to a unit bubble. As is well known [6], the boiling process in a heterogeneous system commences after formation of a wall layer of superheated liquid of sufficient thickness d. Due to the energy contained in this superheated layer there appear on the heat liberation surface nuclei of critical size, at the base of which a liquid microfilm is formed. With increase in bubble radius the interphase surface of its cupola displaces the upper wall layer of superheated liquid (Fig. 1). This leads to "baring" of a superheated microfilm on the heat liberation surface. This microfilm proves to be in a deeply metastable state and evaporates intensely. Since its enthalpy is insufficient to reestablish thermodynamic equi-

Dagestan Polytechnic Institute. Geothermic Problems Institute, Dagestan Filial, Academy of Sciences of the USSR, Makhachkala. Translated from Inzhenerno-Fizicheskii Zhurnal, Vol. 61, No. 1, pp. 92-97, July, 1991. Original article submitted April 23, 1990.

 0022-0841/91/6101-0880$12.50

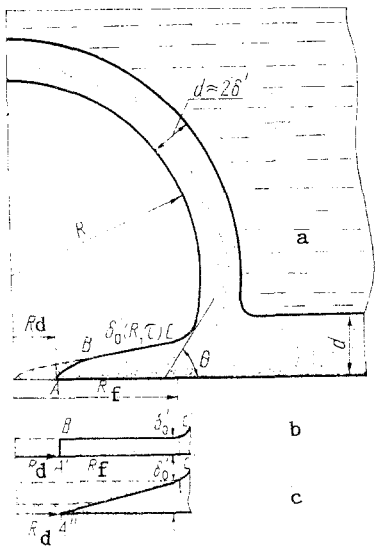

Fig. 1. Schematic bubble section. Higher point concentration corresponds to higher temperature: a) real form of microfilm; b, c) simplified.

librium, a dry spot is formed beneath the bubble. Moreover, a layer of liquid of thickness δ', adjacent to the bubble cupola, is cooled to the vapor temperature due to evaporation over the time required for generation of a critical nucleus, while it follows from the experimental data of [13] that δ' is larger than the thickness of the microfilm [$(2\text{-}3)\cdot10^{-6}$ m], while the temperature head across the liquid layer adjacent to the bubble interphase boundary is less than that across the microfilm.

As shown in Fig. 1a, the liquid microfilm beneath the bubble has a complex radial section. For simplification of the calculations we will consider two limiting cases: A'B'C' (Fig. 1b), a microfilm of constant thickness, gradually evaporating from the center of the bubble base; A"C" (Fig. 1c), the thickness of the remaining portion of the microfilm grows linearly from the periphery of the bubble base. The evaporation portion of the microfilm is hatched in the figures.

Considering the above, the equations of mass balance and vapor energy in the bubble and microfilm can be written in the form

$$\rho' dV = \rho\,[2\pi R_d \delta dR_d + \pi (R_f^2 - R_d^2)\, d\delta], \tag{1}$$

$$\lambda \frac{\partial T}{\partial \delta} S_f = \rho' r' \frac{dV}{d\tau}. \tag{2}$$

The left side of Eq. (1) is the mass of vapor in the bubble, the first term on the right is due to growth in the dry spot, and the second considers change in the thickness of the remaining portion of the microfilm, the quantity

$$S_f = \pi (R_f^2 - R_d^2) \tag{3}$$

is the instantaneous area of the microfilm.

In Eqs. (1), (2) the bubble volume is defined by the expression

$$V = \frac{1}{4}\pi R^3 \psi(\theta),$$

where $\psi(\theta) = 2 + 3\cos\theta - \cos^3\theta$.

Assuming a hemispherical bubble form with fixed center, for the radius of the external boundary of the microfilm we have:

$$R_f = R \sin\theta. \tag{4}$$

Initial and boundary conditions are as follows:

$$R = r_0,\ \delta = \delta_0',\ T = T_c,\ R_d = 0 \quad \text{if} \quad \tau = 0,$$

$$R = R_0,\ \delta = 0,\ T = T_d,\ R_d = R_f \quad \text{if} \quad \tau = \tau_0.$$

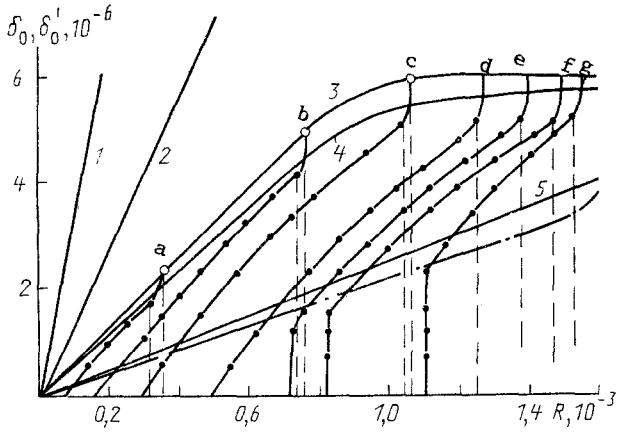

Fig. 2. Comparison of calculated and experimental values of microfilm thickness beneath growing bubble; 1) calculation by equation of [8]; 2) [10]; 3) [9]; 4) experiment [9]; 5) Eq. (9a). Experimental values of instantaneous liquid microfilm profiles for various bubble growth times denoted by points: a) τ = 0.1 msec; b) 0.5; c) 1.3; d) 2.5; e) 3.7; f) 4.9; g) τ = 6.1 msec. δ_0, δ_0' m; R, m.

In the first model the microfilm thickness is constant. Then in Eq. (1) we drop the second term on the right. In solving Eqs. (1) and (2) the instantaneous microfilm area is replaced by its mean value. From Eqs. (1) and (2) we obtain the following expressions for the thickness of the evaporating microfilm and radius of the dry spot:

$$\delta_0' = (\mathrm{Ja}\rho'/2\rho)^{1/2}\sqrt{a\tau}, \tag{5}$$

$$R_d = \left(\frac{2\rho'}{8\,\mathrm{Ja}\,\rho}\right)^{1/4}\sqrt{\psi(\theta)}\,[\varphi^3(\mathrm{Ja})\,a\tau - r_0^3/\sqrt{a\tau}]^{1/2}. \tag{6}$$

Here δ_0' and R_d are expressed as functions of time. Their dependence on bubble radius can be written as:

$$\delta_0' = (\mathrm{Ja}\rho'/2\rho)^{1/2}R/\varphi(\mathrm{Ja}), \tag{5a}$$

$$R_d = [\psi(0)\rho' R^3/3\rho\delta_0']^{1/2}. \tag{6a}$$

In Eq. (6a) we have dropped the small correction $r_0^3/\sqrt{a\tau}$ and taken the bubble radius equal to [7]

$$R = \varphi(\mathrm{Ja})\sqrt{a\tau}, \tag{7}$$

where $\varphi(\mathrm{Ja}) = 0.3\mathrm{Ja} + \sqrt{0.09\mathrm{Ja}^2 + 12\mathrm{Ja}}$.

In the second case, after simple transformations we have:

$$R_d = \left[\frac{\psi(\theta)\rho'}{\delta_0'\rho}(R^3 - r_0^3) - 3R_f^2/4\right]^{1/2} - \frac{R_f}{2}. \tag{8}$$

Equation (8) was obtained on the assumption that over the time τ_0 the microfilm evaporates in the form of a section of a cone of liquid (Fig. 1c) with major radius equal to R_f and minor radius R_d. The thickness of the microfilm at point r is:

$$\delta_0(r) = \delta_0'(R_f - r)/(R_f - R_d).$$

To test the expression obtained and compare them to relationships proposed by other researchers [8-10], calculations were compared to experimental data from [9]. Figure 2 shows experimental and theoretical values of microfilm thickness for boiling of dichloromethane [9]. Shown are calculated graphs using expressions presented in [8] (curve 1), [10] (curve 2), curve 3 corresponds to the calculated data of [9], curve 4 is experimental maximum microfilm

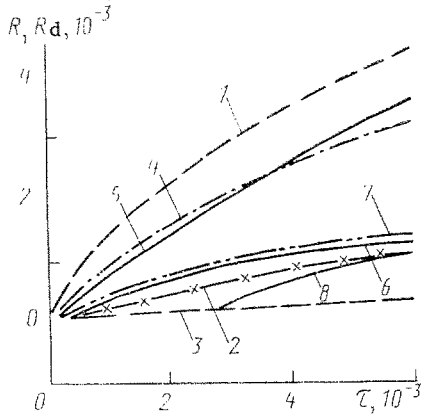

Fig. 3. Calculated bubble and dry spot radius vs. time for dichloromethane: 1) bubble radius; 2) experimental dry spot radius values [9]; 3) Dwyer equation with microfilm thickness after [8]; 4) Eq. (6a); 5) Eq. (6a) with τ_0 = 6 msec; 6) Dwyer equation with δ_0' using Eq. (5a); 7) Eq. (8); 8) Eq. (8) with τ = 6 msec. τ, sec; R, R_d, m.

TABLE 1. Calculated Vapor Bubble Parameters

Parameters	Water		Toluene		Methyl alcohol	
ΔT, K	1	5	1	5	1	5
Ja	3,10	15,00	1,35	6,74	1,59	7,97
φ (Ja)	6,96	18,65	4,45	11,24	4,88	12,46
l_0, mm	1,21		0,883		0,963	
δ_0', μm	5,31	4,43	9,95	8,82	7,13	6,25
δ', μm	81	53	20	12	98	57

thickness values, curve 5 is a calculation of mean thickness with Eq. (5a), and finally, the dash-dot line describes averages over to area of the experimental data of [9]. The solid lines show instantaneous microfilm profiles at certain times τ. As is evident from the figure, Eq. (5a) describes the experimental data for mean microfilm thickness satisfactorily. Verifying the correspondence of Eq. (5a) to the experimental results of [11, 12] is complicated by the absence of sufficient data on the conditions under which the experiments were performed.

It should be noted that the liquid microfilm thickness also depends on the structure of the heat liberation surface. For a rough structure the microfilm thickness increases in proportion to the height of microroughnesses. The dry spot radius then decreases in inverse proportion to the square root of δ_0'. For a precise calculation of the quantities R_d and δ_0' at thermal flux densities close to critical, it is necessary to also consider the fraction of heat supplied to the bubble through the dry portion of the surface underlying the bubble [14-16]. This is true because at high temperature heads the superheating of the dry sections reaches perceptible values [13].

Evidence in favor of the heat liberation mechanism described in the growing bubble is the fact that the thickness δ' of the cooled liquid layer adjacent to the bubble cupola is much greater than the thickness of the microfilm δ_0'. To test this assertion we will use the expression for thickness of the superheated liquid layer from [17]: $d = 2.88(a_v/\Delta T\beta g)^{1/2}$. This expression is valid for high superheats and yields artificially low values of d for low superheating on the heat liberation surface, in which case one can use the expression proposed in [18], which yields even higher values of d. We will take the quantity δ' approximately equal to half the thickness of the wall thermal layer, "extended" above the bubble cupola.

Table 1 shows values of microfilm and cooled layer thickness adjacent to the interphase boundary of the bubble dome for boiling of water, toluene, and methyl alcohol under normal conditions. The breakoff radius was determined by the expression of [19]

$$R_0 = k\left|\sigma(c_p T_c/\rho' r')^{5/2}/g(\rho - \rho')\right|^{1/2},$$

where $k = 2.325 \cdot 10^{-4}$ for water, $k = 0.75 \cdot 10^{-4}$ for the other liquids. Wall superheating was taken equal to 1 and 5 K, and boiling was assumed stable. As is evident from Table 1, the quantity δ' is an order of magnitude greater than the thickness of the microfilm. Consequently, the thermal resistance of the microfilm is much less than the resistance of the cooled layer.

Figure 3 shows calculations of the dry spot radius for boiling of dichloromethane by Eqs. (6a), (8), and the Dwyer relationship [20]:

$$R_d = R/\sqrt{1+(\delta_0'/RS_{1/2})^2},$$

where

$$S_{1/2} = \rho'/\rho\,[1+(3\lambda c\rho/\lambda_\omega \overset{d}{c}_\omega \rho_\omega)^{1/2}].$$

For the bubble radius (curve 1) an equation from [9] was used. Curve 2 corresponds to an experimental dry spot profile. Substitution in the Dwyer equation [20] of the Cooper–Lloyd expression [8] for microlayer thickness yields lowered values of dry spot radius (curve 3). Equation (6a) produces an elevated result (curve 4). Assuming the microfilm thickness constant over time and equal to the value corresponding to a breakoff time τ_0 = 6 msec, we obtain curve 5 for the dry spot radius. Substitution in Dwyer's equation of δ_0' from Eq. (5a) (curve 6) yields results close to those of Eq. (8) (curve 7).

Moreover, Fig. 3 also shows a curve of dry spot radius 8 with consideration of τ_0. In the period from 0 to 2.2 msec $R_d < 0$. This can apparently be explained by a flow of liquid under the bubble at microfilm supply rates exceeding the relative bubble growth rate because of surface tension forces. This also explains the results of Sharp [12], who maintained that a dry spot appears some time after generation of the bubble – after evaporation of a portion of the microfilm at the vapor formation center. An exact knowledge of the form $\delta_0(\tau, r)$ would be required to refine the model in this region.

Thus, it can be stated that the mechanism of heat supply to the bubble through the interphase boundary of its dome can be neglected in a heterogeneous system. This also permits a more proper expression for the bubble radius for simultaneous solution of the corresponding system of differential equations.

As is evident from the comparative analysis of results of Eqs. (6), (8) with available experimental data and the equations of other authors, the mechanism of energy supply to a bubble in a heterogeneous system described above produces a good correspondence to the real pattern of the phenomenon. The calculation expressions for microfilm thickness and dry spot radius contain no semiempirical constants and satisfactorily describe the experimental data of [9].

NOTATION

T, T_s, T, $\Delta T'$, instantaneous temperature, temperature of heat liberation surface, vapor saturation temperature in bubble, temperature head across microfilm; δ, δ_0', δ_0, δ', and d, instantaneous and final values of microfilm thickness beneath bubble, corresponding to first and second models, cooled layer thickness on interphase boundary of cupola, and superheated liquid wall film; τ and τ_0, actual time and time of bubble growth to breakoff size; r_0, R_d, R_d', R, R_0, and R_f, critical nucleus radius, instantaneous and breakoff values of dry spot, instantaneous and breakoff bubble radius, microfilm radius; ρ, ρ', and ρ_ω, density of vapor, liquid, and heat liberation surface; λ and λ_ω, thermal conductivities of liquid and heat liberation surface; σ, surface tension coefficient; θ, wetting angle; Ja, Jacobi criterion; S_f, microfilm surface; a, liquid thermal diffusivity; r', specific heat of vapor formation; c and c_ω, specific heats of liquid and heat liberation surface.

LITERATURE CITED

1. M. S. Plezet and S. A. Tsvik, Questions in the Physics of Boiling [in Russian], Moscow (1964), pp. 189-211.
2. G. Forster and N. Zubr, Questions in the Physics of Boiling [Russian translation], Moscow (1969), pp. 212-225.
3. D. A. Labuntsov, Inzh. Fiz. Zh., 6, No. 4, 33-39 (1963).
4. V. I. Tolubinskii, Heat Exchange in Boiling [in Russian], Kiev (1980).
5. I. N. Il'in, S. R. Yaundalger, and M. I. Khesin, Thermophysics and Gas Hydrodynamics of Boiling and Condensation Processes. Materials of the All-Union Conference, Riga, 1982, Vol. 1, Bubble Boiling, Part 2 [in Russian], Riga (1985), pp. 103-119.
6. Heat Exchanger Handbook [in Russian], Vol. 1 [in Russian], Moscow (1987).
7. V. V. Yagov, "Liquid boiling in the low pressure region," Author's Abstract of Candidate's Dissertation [in Russian], Moscow (1971).

8. M. G. Cooper and A. J. L. Lloyd, Int. J. Heat Mass Transf., 12, 895-913 (1969).
9. J. Watsin, Teploperedach., No. 1, 89-94 (1975).
10. W. Olender, Teploperedach., No. 1, 149-156 (1969).
11. H. H. Jawurek, Int. J. Heat Mass Transf., 12, 843-848 (1969).
12. Sharp, "The nature of liquid film evaporation during nucleate boiling," NASA TN D-1997 (1964).
13. N. Afgan, Superheating of Boiling Liquids [in Russian], Moscow (1979).
14. M. G. Verdiev, "Physics of heat-mass exchange processes in condensation of sealed evaporation-condensation heat transport equipment," Dep. VINITI, No. 3978-V88, May 26, 1988.
15. M. G. Verdiev, "Physical and mathematical model of heat-mass exchange processes in liquid boiling," Dep. VINITI, No. 5124-V88, June 27, 1988.
16. M. G. Verdiev and S. A. Ninalalov, "Use of data banks for regional studies," Reports to the International Symposium, Makhachkala (1988).
17. A. I. Leon'tev and A. G. Kirdyashkin, Inzh. Fiz. Zh., 16, No. 6, 1110-1115 (1969).
18. I. N. Ilyin, V. P. Grivtsov, and S. R. Jaudalddere, Proc. 7th Internat. Heat Transf. Conf., Munich, Vol. 4 (1982), pp. 55-59.
19. V. Rozenov, Heat Transfer at Low Temperatures [in Russian], Moscow (1977), pp. 122-160.
20. O. Dwyer, Heat Exchange in Boiling of Liquid Metals [Russian translation], Moscow (1980).

KINETICS OF THE SOLUTION OF MINERAL SALTS SUSPENDED IN A LIQUID FLOW

G. A. Aksel'rud, A. E. Boiko, and A. E. Kashcheev

UDC 532.73-3

Results are presented from an experimental study on determination of the mass liberation coefficient from particles of mineral salts suspended in a liquid flow. The experimental data are generalized in the form of a criterial equation which adequately describes the mass liberation coefficients. It is established that in analyzing the kinetics of mineral salt solution it is necessary to consider the changes in viscosity and density of the solution and the diffusion coefficients within the diffusion layer. The time required for exit to a diffusion regime of solution is estimated and the validity of using Eq. (4) to process experimental data is evaluated using the diffusion number Fo.

As has been demonstrated by Zdanovskii [1], the majority of mineral salts dissolve in a diffusion regime, in which the rate of solution is determined by the equation

$$-dM/d\tau = kF(C_s - C). \tag{1}$$

The diffusion rate coefficient K is of key significance, and under diffusion solution conditions that quantity is identical to the mass liberation rate. Numerous experimental values of the coefficient K have been established and are presented in [2]. A number of studies have presented methods for generalizing experimental data on the diffusion rate coefficient [3, 4].

For solid particles of mineral salts suspended in an incident liquid flow (rectilinear and uniform) such a generalization was performed by Aksel'rud, and independently by Zdanovskii. This generalization can be expressed in the form

$$\mathrm{Sh} = 0.31 \sqrt[3]{\mathrm{Sc}}\sqrt[3]{\mathrm{Ar}}. \tag{2}$$

For a single individual salt with various particle dimensions this equation adequately describes the experimental data, the proportionality $\mathrm{Sh} \sim \sqrt[3]{\mathrm{Ar}}$ being observed, but experimental data on solution of a group of salts cannot be generalized with Eq. (2).

Lenin Komsomol Polytechnic Institute, L'vov. Translated from Inzhenerno-Fizicheskii Zhurnal, Vol. 61, No. 1, pp. 98-102, July, 1991. Original article submitted May 21, 1990.